Real-Time Sleep Apnea Detection by Classifier Combination

Baile Xie, *Student Member, IEEE*, and Hlaing Minn, *Senior Member, IEEE*

***Abstract*—To find an efficient and valid alternative of polysomnography (PSG), this paper investigates real-time sleep apnea and hypopnea syndrome (SAHS) detection based on electrocardiograph (ECG) and saturation of peripheral oxygen (SpO_2) signals, individually and in combination. We include ten machine-learning algorithms in our classification experiment. It is shown that our proposed SpO_2 features outperform the ECG features in terms of diagnostic ability. More importantly, we propose classifier combination to further enhance the classification performance by harnessing the complementary information provided by individual classifiers. With our selected SpO_2 and ECG features, the classifier combination using *AdaBoost with Decision Stump*, *Bagging with REPTree*, and either *kNN* or *Decision Table* achieves sensitivity, specificity, and accuracy all around 82% for a minute-based real-time SAHS detection over 25 sleep-disordered-breathing suspects' full overnight recordings.**

***Index Terms*—Classifier combination, electrocardiograph (ECG), feature selection, hypopnea, machine learning, saturation of peripheral oxygen (SpO_2), sleep apnea.**

I. Introduction

SLEEP apnea and hypopnea syndrome (SAHS) is a common sleep disorder which is characterized by abnormal breath pause or reduction during sleep. It is estimated to affect 2% of middle-aged women and 4% of middle-aged men [1]. Sleep apnea is treatable; however, about 90% of sufferers go unidentified and hence untreated [2]. They experience daytime sleepiness and fatigue which can escalate to traffic accidents, depression, and memory loss. Moreover, untreated SAHS can also relate to ischemic heart disease, cardiovascular disfunction, and stroke [3], [4]. A common definition of apnea involves a cessation of airflow for at least 10 s while hypopnea is defined as a minimum 10-s airflow reduction with either a blood oxygen desaturation of 4% or a neurological arousal [5]. Currently, polysomnography (PSG) is considered as the standard method for SAHS diagnosis. Nevertheless, PSG requires SAHS suspects to sleep in a sleep laboratory over one or two nights, with attended technicians. During the overnight sleep, a variety of sensors and wires are attached to the suspect's body. The recorded signals are then analyzed by sleep specialists for final diagnosis. The discomfort, inconvenience, and expensiveness of PSG set a barrier from its prevalence among public. Therefore, a readily available, relatively inexpensive, and reliable diagnosis alternative is desirable for public use.

In the past decade, several methods have been proposed as PSG alternatives for SAHS detection. For instance, detections have been developed based on questionnaires [6], snoring [7], electrocardiograph (ECG) [8]–[12], and pulse oximetry [5], [12]–[21]. Among them, ECG and saturation of oxygen measured by pulse oximeter (SpO_2) are the two most extensively studied signals.

Specifically, based on the ECG signal alone, various frequency and time domains as well as ECG morphology features have been developed. For example, McNames and Fraser [8] found that the heart rate (HR), the S-pulse amplitude, and the pulse energy of the ECG signal are informative for SAHS detection. Raymond *et al*. [9] analyzed the power spectral features of the ECG-derived respiration (EDR) signal via wavelet transform in addition to other features from the RR interval tachogram. Shinar *et al*. [10] extracted features from the changes of ECG signal's QRS complex and spectral abnormalities of heart rate variability (HRV).

SpO_2 is the percentage (%) of hemoglobin in the blood that is saturated with oxygen recorded by a pulse oximeter. Some commonly used SpO_2 features are the accumulative time (*TSA*) spent below a certain saturation level [5], [14], the oxygen desaturation index (*ODI*, the number of oxyhemoglobin desaturation below a certain threshold) [15], and the saturation variability index (*Delta index*) [5], [13], [14]. Later on, several nonlinear parameters such as approximate entropy (*ApEnt*) [16], central tendency measure (*CTM*), and Lempel–Ziv complexity (*LZCom*) [17] were also applied to sleep apnea detection. In the realm of spectral-domain features, Zamarrón *et al*. [18] studied the periodogram of the SpO_2 signal and selected four indices related to the period 30–70 s for detection purpose. However, all the aforementioned methods rely on the entire overnight SpO_2 records, resulting in a delayed offline analysis and diagnosis.

In order to obtain a real-time SAHS monitoring and diagnosis, some pioneering works have emerged. Oliver and Flores-Mangas [19] implemented a real-time detection system with oximetry but unfortunately lacked a performance comparison with the standard PSG. Heneghan *et al*. [12] adopted both ECG and SpO_2 signals to estimate the apnea plus hypopnea index (AHI) based on an epoch-by-epoch detection. Most recently, Burgos *et al*. [20] and Bsoul *et al*. [11] have implemented a systematic real-time SAHS detection based on SpO_2 alone and ECG alone, respectively.

In this paper, we focus on real-time sleep apnea/hypopnea detection based on 1-min segments of ECG and SpO_2 signals. While following the comprehensive ECG features set in [11], we

Manuscript received April 21, 2011; revised September 23, 2011 and January 19, 2012; accepted February 9, 2012. Date of publication February 16, 2012; date of current version May 4, 2012.

The authors are with the Department of Electrical Engineering, University of Texas at Dallas, Richardson, TX 75080 USA (e-mail: baile.xie@utdallas.edu; hlaing.minn@utdallas.edu).

Digital Object Identifier 10.1109/TITB.2012.2188299

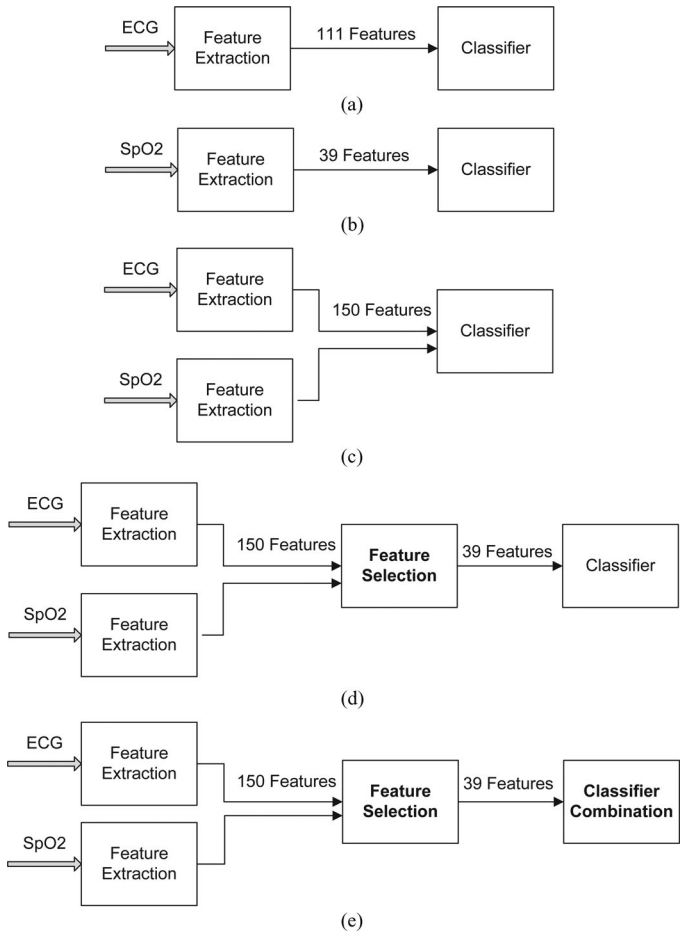

Fig. 1. Different strategies of SAHS detection. (a) SAHS detection based on the ECG signal only. (b) SAHS detection based on the SpO_2 signal only. (c) SAHS detection based on both ECG and SpO_2 signals. (d) SAHS detection based on ECG and SpO_2 signals with feature selection. (e) SAHS detection based on selected ECG and SpO_2 features with classifier combination.

develop an SpO_2 feature set of 39 features. The different strategies of SAHS detection that we explore can be found in Fig. 1. To begin with, investigations of individual diagnostic abilities of the ECG and SpO_2 features are carried out and compared via an experiment of ten different machine-learning algorithms. Cost-sensitive classification is included to enhance the sensitivity. Additionally, the classification experiment extends to involving a full set of 150 features fused by both ECG and SpO_2 features. In contrast to feature selection based on individual evaluation of each feature as used in existing works [11], [20], [21], we utilize a subset feature selection strategy that accounts not only the prediction ability of each feature, but also the redundancy among features. The idea of cost-sensitive weighting is also incorporated in the feature selection process to favor highly predictive features. Most importantly, with investigation of the performances of individual classifiers, we introduce classifier combination to further enhance detection performance by harnessing the potentially complementary information provided by individual classifiers.

The rest of this paper is organized as follows. In Section II, we describe the database and the methods used in our experiment, including signal processing, feature extraction, feature selection, and classifier combination. Section III shows the results of different classification strategies. In Section IV, we discuss the performances among different feature sets and classification schemes, and compare our results with those of other research groups. Finally, Section V concludes this paper.

TABLE I
PHYSIOLOGICAL PROPERTIES OF SUBJECTS IN UCD DATABASE

	Mean Value	Range
Age	50 ± 10 years	28 - 68 years
Body Mass Index	31.6 ± 4.0 kg/m^2	25.1 - 42.5 kg/m^2
AHI	24.1 ± 20.3	1.7 - 90.9

II. MATERIALS AND METHODS

A. Database

Throughout this paper, we use the St. Vincent's University Hospital/University College Dublin Sleep Apnea Database (UCD database) [22] available online from PhysioNet [23] which provides a variety of physiological signals for biomedical research. The availability of the *UCD database* offers easy validation and assessment of our approach. Twenty-five (21 males and 4 females) sleep-disordered-breathing suspects' full overnight PSG recordings are recorded in the database. Each recording contains 5.9- to 7.7-h ECG and SpO_2 signals as well as an annotation file with detailed onset time and duration of every apnea/hypopnea event. Polysomnograms were obtained using the Jaeger–Toennies system (Erich Jaeger GmbH, Germany). In particular, the ECG signal was recorded via a modified lead V2 and the SpO_2 signal was recorded using a finger pulse oximeter. General physiological properties of the subjects are listed in Table I while a more detailed description can be found online [22].

B. Signal Processing and Feature Extraction

The ECG and SpO_2 signals in the database are originally sampled by 128 and 8 Hz, respectively. In our experiment, both signals are segmented into 1-min episodes for signal processing and the detection/classification results are returned minute by minute. Accordingly, the annotations need to be modified to give minute-based references. Given that the apnea/hypopnea happens with a minimum of 10-s airflow change, in case the events are across two adjacent segments, we label a single minute as "Apnea" (apneic) if it contains at least 5 consecutive seconds of apnea/hypopnea events; otherwise, this minute is annotated as "No apnea" (normal). We use MATLAB for signal processing and feature extraction.

Recently, Bsoul *et al*. [11] have proposed a quite comprehensive ECG feature set which contains 111 HRV- and EDR-based features in both time and spectral domains. In this paper, we employ this feature set for the ECG signal and mainly focus on feature designs of the SpO_2 signal due to its strong reflection of arterial oxygen saturation on the airflow fluctuation.

To begin with, the SpO_2 signal is downsampled at 1 Hz. Any SpO_2 values less than 50 are considered as artifacts and hence

removed from analysis (totally about 137 min; 1.3% of data are removed).

Basic statistics such as the minimum, mean, variance, and correlation coefficient of SpO_2 samples within each segment are first calculated and denoted as *Smini, Smean, Svari*, and *CorreC*, respectively. Then using *Smean* as a baseline, the number of zero crossing points of each segment is counted as feature *NumZC*. Within each segment, via linear regression, a regression line is fitted. The *Slope*, its absolute value (*AbSlope*), and *Bias* of the regression line are measured as three additional features.

Delta index is viewed as a valid parameter for overnight SAHS detection [5], [13], [14]. In our real-time processing, the mean value of the SpO_2 signal over every 12-s interval is first computed and the Delta index (*Dmean*) is derived as the one-min average of the absolute differences between two successive mean values.

The nonlinear methods such as *ApEnt*, *CTM*, and *LZCom*, which measure the regularity, variability, and complexity of a time series, have been applied to SAHS detection based on overnight SpO_2 signals [16], [17]. These three features can also be easily calculated segmentwise. In particular, for *ApEnt*, we choose the optimal run length of 1 and tolerance window of 0.25 times the standard deviation of each epoch data, as suggested in [16]. The *CTM* is calculated by selecting a radius with respect to (w.r.t.) the origin of a second-order difference plot and counting the number of points which fall within the radius [17]. We choose radii of 0.25, 0.5, 0.75, and 1, corresponding to features *CTM25*, *CTM50*, *CTM75,* and *CTM100*, respectively.

Besides three ODI indices (*odi2*, *odi3*, *odi4*) in [20], we adopt a more general definition of ODI indices as in [15]. We set the baseline as the mean of the top 20% of the SpO_2 data within 1 min. The ODI index *ODIxy* counts the occurrences that SpO_2 samples drop at least x below the baseline and last at least y s. In our experiment, $x \in \{2, 3, 4, 5\}$ and $y \in \{1, 3, 5\}$. For example, *ODI21* presents the number of times when the SpO_2 level declines at least 2 below the baseline and lasts at least 1 s. Additionally, we count the total number of SpO_2 samples which fall at least 2, 3, 4, and 5 below the baseline, contributing another four features: *ODIS2, ODIS3, ODIS4*, and *ODIS5*.

Finally, we consider five TSA indices (*tsa95*, *tsa90*, *tsa85*, *tsa80*, *tsa70*) indicating the accumulative time that the SpO_2 level stays below 95, 90, 85, 80, and 70, respectively.

As a result, totally, a set of 39 SpO_2 features is built.[1] The aforementioned SpO_2 features and their descriptions are summarized in Table II for ease of reference.

TABLE II
SpO_2 FEATURES AND THEIR DESCRIPTIONS

Feature Name	Description
Smini	Minimum of 1-minute SpO_2 samples
Smean	Mean value of 1-minute SpO_2 samples
Svari	Variance of 1-minute SpO_2 samples
CorreC	Correlation coefficient of 1-minute SpO_2 samples
NumZC	Number of zero crossing points within 1-minute SpO_2 samples, using *Smean* as baseline
Slope	Slope of the regression line fitted for 1-minute SpO_2 samples
AbsSlope	Absolute value of *Slope*
Bias	Bias of the regression line fitted for 1-minute SpO_2 samples
Dmean	Delta index: 1-minute average of the absolute differences between two successive mean values of SpO_2 signal over 12-second intervals
ApEnt	Approximate entropy [16] with run length of 1 and tolerance window of $0.25\sqrt{Svari}$
LZCom	Lempel-Ziv complexity [17]
CTM25, *CTM50*, *CTM75*, *CTM100*	Central tendency measure [17] with radius $0.25, 0.50, 0.75, 1.00$ (calculated by selecting a radius w.r.t. the origin of a second-order difference plot and counting the number of points that fall within the radius)
odi2, *odi3*, *odi4*	Oxygen desaturation index defined in [20]
ODIxy, $x \in \{2, 3, 4, 5\}$, $y \in \{1, 3, 5\}$	The number of occurrences that SpO_2 level declines at least x below the baseline and lasts at least y seconds (The baseline is the mean value of the top 20% of the SpO_2 data within 1 minute.)
ODIS2, *ODIS3*, *ODIS4*, *ODIS5*	The total number of SpO_2 samples that fall at least $2, 3, 4, 5$ below the baseline (The baseline is the mean value of the top 20% of the SpO_2 data within 1 minute.)
tsa70, *tsa80*, *tsa85*, *tsa90*, *tsa95*	Accumulative time that SpO_2 level stays below $70, 80, 85, 90, 95$

C. Classification

In the classification phase, we employ an open-source machine-learning software, WEKA [24], as the major tool to assess the performances of the aforesaid feature sets. Ten classifiers are included in our experiments. Specifically, support vector machine (SVM) [25] maps data into a high-dimensional space and constructs a hyperplane to separate them. *k*-nearest neighbor (*k*NN) [26] assigns the data the most common class among their k closest neighbors. *Decision Table* classifier [27] builds a simple hypothesis space represented by a decision table and uses it for classification. Multilayer perceptron (MLP) [28] is an artificial neural network consisting of multiple layers of nodes; it models data pattern during training and follows the pattern to classify the testing data. *Decision tree* partitions data into different groups recursively. Several popular decision trees and their evolved versions are included, such as *C4.5 tree* [29], *reduced-error pruning tree (REPTree)*, and *functional trees (FT trees)* [30]. We also take into consideration several meta-algorithms which are used in conjunction with other (simple) classifiers to reduce prediction errors. In particular, *Adaptive Boosting (AdaBoost) with Decision Stump* [31], *Bagging with REPTree* [32], and *Bagging with Alternating Decision Tree (ADTree)* [33] are included in our experiment.

Throughout the experiment, the default parameter settings of each classifier are kept, except that for SVM; we normalize all the features into the $[0, 1]$ region since SVM is sensitive to the dynamic ranges of the features. And for *kNN* classifier, we choose $k = 5$ and apply an inverse distance weight function.

To assess the classification performance, we use sensitivity, specificity, and accuracy as evaluation metrics. Their definitions are as follows:

$$\text{sensitivity} = \frac{\text{TP}}{\text{TP} + \text{FN}} \tag{1}$$

[1]We mainly focus on the time-domain features in our real-time processing since the apnea/hypopnea event can last as long as 120 s [19], which exceeds the epoch length. Part of the SpO_2 features is used in our conference paper [21].

$$\text{specificity} = \frac{\text{TN}}{\text{TN} + \text{FP}} \tag{2}$$

$$\text{accuracy} = \frac{\text{TP} + \text{TN}}{\text{P} + \text{N}} \tag{3}$$

where true positive (TP) and true negative (TN) refer to the number of correctly detected apneic epochs and normal epochs, respectively, whereas false positive (FP) and false negative (FN) stand for the number of miss-identified apneic and normal epochs, respectively. *P*/*N* represents the total number of epochs with/without apneic events. In other words, the sensitivity reflects the ability to correctly detect the apneic epochs; specificity conveys the ability to distinguish the normal epochs. A tradeoff between the two usually exists in practice. In terms of SAHS detection problem, we are more interested in high sensitivity algorithms which reduce the risk of missing the apnea/hypopnea events that do pose threats to the patients. Therefore, we also carry out cost-sensitive classifications by imposing a cost matrix on the above ten classifiers, to penalize the FN errors more than the FP errors, and aim for a higher sensitivity.

As can be seen in Fig. 1, we first carry out experiments to assess and compare the individual diagnostic abilities of ECG and SpO_2 features. The 111 ECG features and 39 SpO_2 features are fed into the ten classifiers, respectively [see Fig. 1(a) and (b)]. In the next experiment, we fuse the two feature sets together and perform classification with a full set of 150 features [see Fig. 1(c)]. The experiments include both even cost (where the FN and FP are evenly weighted) and cost-sensitive classifications.

Note that all the experiment results are based on tenfold cross validation of the entire database. In particular, the entire dataset is evenly divided into ten folds; each time, one fold is left out for testing while the other nine folds are used for training. The testing results are averaged over ten folds and then returned as the final cross-validation results.

D. Feature Selection

Feature selection is regarded as a classic method to prevent overfitting by eliminating redundant or even detrimental features. In a real-time detection scenario, it is also an effective way to reduce the computational load by requiring less signal processing in feature extraction, to lower the rate of data transmission and energy consumption, and more importantly, to shorten the time required for model building during the training process.

Feature selection can be done by either investigating the value of each features, as done in [11], [20], and [21], or using a subset evaluator to assess the merit of a group of features. With the former method, no interinformation among features can be concluded, whereas the latter strategy can explore the correlation among features. Therefore, we employ the latter subset feature selection to further reduce redundancy.

In the interest of high sensitivity, we also use a cost-sensitive subset evaluator for feature selection. Cost-sensitive subset evaluator is a meta subset evaluator which requires a base subset evaluator and a cost matrix. In our case, the same cost matrix used in cost-sensitive classification is applied, and thus, the features with higher sensitivity are preferred. In terms of the base subset evaluator, correlation-based feature subset selection (CfsSubsetEval) [34] is employed independently of classifiers. CfsSubsetEval evaluates the merit of a subset of features by considering the individual predictive ability of each feature as well as the redundancy among them. To be specific, the merit of a subset S is calculated as [34]

$$M_S = \frac{k\overline{r_{\text{cf}}}}{\sqrt{(k + k(k-1)\overline{r_{\text{ff}}})}} \tag{4}$$

where k is the number of features in S; $\overline{r_{\text{cf}}}$ is the average class-feature correlation while $\overline{r_{\text{ff}}}$ is the average feature–feature intercorrelation. As a result, a subset of features which are highly correlated with the class (apneic or normal) while having low intercorrelation among the features is preferred. In our experiment, feature selection is performed on the full feature set which consists of 111 ECG and 39 SpO_2 features.

E. Classifier Combination

Naturally, one would want satisfactory results in all sensitivity, specificity, and accuracy. However, this ideal result does not always happen given a single classifier. Some classifiers provide high sensitivity but low specificity while others perform the opposite way. The gap between the two metrics can be large. To strike a balance, classifier combination is proposed as a potential solution.

Classifier combination has been proved to be a powerful method to improve the classification performance in many fields [35]. Inspired by the fact that the misclassified instances of individual classifiers do not necessarily overlap, different classifiers may offer different perspectives in decision making. Making use of those complementary information by classifier combination could further improve the performance.

In our combination experiment, we choose three individual classifiers to form a group of experts. Each member classifier predicts the class of every epoch and records the probabilities associated with both classes (apneic and normal). Since the *prior* class distribution of a database is usually unaware beforehand, an equiprobable *prior* is a common assumption. Based on the predicted classes and their corresponding probabilities, we explore four classifier combination schemes as described next.

1) Max Probability (MP): This scheme assigns the predicted class as the one with the maximum probability among all classifiers and classes:

$$C_p = \arg \max_{\{C+,\, C-\}} \max_i \{P_i(C+), P_i(C-)\} \tag{5}$$

where C_p is the final predicted class after combination and i is the classifier index. $P_i(C+)$ and $P_i(C-)$ are the probabilities that classifier i predicts the epoch to be positive (apneic) and negative (normal), respectively.

2) Average Probability (AP): In this rule, the probabilities of the positive/negative class are summed over all classifiers (can be viewed as the arithmetic mean criterion). The class with

TABLE III
CLASSIFICATION RESULTS BY USING EITHER ECG OR SpO_2 FEATURE SET

	Even Cost						Cost Sensitive 3					
	Sensitivity(%)		Specificity(%)		Accuracy(%)		Sensitivity(%)		Specificity(%)		Accuracy(%)	
Classifier	ECG	SpO_2	ECG	SpO_2	ECG	SpO_2	ECG	SpO_2	ECG	SpO_2	ECG	SpO_2
SVM	0.00	54.00	100.00	94.10	75.66	84.36	66.99	78.18	72.78	82.84	71.37	81.70
C4.5 tree	47.56	60.47	85.66	90.41	76.39	83.13	53.91	70.31	79.14	83.88	73.00	80.58
Bagging.REPTree	45.49	63.73	92.96	92.40	81.41	85.43	69.82	78.23	**80.29**	**84.25**	**77.74**	**82.79**
Bagging.ADTree	34.15	58.85	93.56	93.94	79.10	85.40	**72.47**	82.74	72.87	80.41	72.77	80.98
FT trees	46.53	59.50	83.73	89.05	74.67	81.86	58.52	72.04	75.43	81.79	71.32	79.42
AdaBoost	31.59	72.64	91.60	87.18	77.00	83.64	67.21	**87.63**	71.08	73.70	70.14	77.09
REPTree	43.54	60.97	90.68	92.53	79.20	84.85	70.47	80.08	74.65	81.11	73.63	80.86
kNN ($k = 5$)	48.53	63.25	90.26	90.92	80.10	84.19	71.17	76.98	77.84	81.19	76.22	80.17
DecisionTable	30.94	59.01	94.46	92.91	79.01	84.66	66.01	80.46	74.00	81.54	72.06	81.28
MLP	30.80	59.17	93.61	91.71	78.32	83.79	61.84	75.68	70.25	83.25	68.20	81.41

TABLE IV
CLASSIFICATION RESULTS BY USING ECG AND SpO_2 FEATURE SETS TOGETHER

	Even Cost			Cost Sensitive 3				
	Sen. (%)	Spe. (%)	Acc. (%)	Sen. (%)	Spe. (%)	Acc. (%)	Training Time (s)	Testing Time (s)
SVM	55.20	94.30	84.74	79.48	83.13	82.24	32.706	2.979
C4.5 tree	63.08	88.72	82.48	67.10	85.35	80.91	4.439	0.002
Bagging.REPTree	65.64	93.35	86.60	79.75	**85.89**	**84.40**	10.399	0.002
Bagging.ADTree	56.90	94.19	85.11	85.13	78.16	79.85	67.453	0.004
FT trees	63.52	87.48	81.65	71.28	81.91	79.32	11.746	3.219
AdaBoost	71.82	87.59	83.75	**87.03**	74.82	77.79	3.154	0.001
REPTree	62.59	92.93	85.55	78.94	82.10	81.33	1.183	0.002
kNN ($k = 5$)	63.74	91.03	84.38	77.69	82.92	81.65	0.000	10.559
DecisionTable	58.63	92.96	84.61	79.75	81.12	80.79	14.043	0.005
MLP	54.62	92.76	83.47	76.27	83.31	81.60	885.532	0.020

larger summed probability is returned as the final prediction:

$$C_p = \arg \max_{\{C+,\, C-\}} \left\{ \sum_i P_i(C+), \sum_i P_i(C-) \right\}. \quad (6)$$

3) Product of Probability (PP): Similar to the aforementioned approach, this scheme chooses the class with the larger product of positive/negative probabilities (can be viewed as the geometric mean criterion):

$$C_p = \arg \max_{\{C+,\, C-\}} \left\{ \prod_i P_i(C+), \prod_i P_i(C-) \right\}. \quad (7)$$

4) Majority Voting (MV): The last approach chooses the class to which the majority of the classifiers agree. Let $C_i(C+) = 1$ if classifier i predicts the current epoch to be positive; otherwise, $C_i(C+) = 0$ and apply a similar rule to $C_i(C-)$. Then, the final prediction is determined as

$$C_p = \arg \max_{\{C+,\, C-\}} \left\{ \sum_i C_i(C+), \sum_i C_i(C-) \right\}. \quad (8)$$

In other words, it compares the numbers of classifiers which give positive/negative predictions, and picks the class with the larger number of votes.

III. RESULTS

A. Results of Individual Classifiers

1) Using Either ECG or SpO_2 Feature Set: The classification results of using either ECG or SpO_2 feature set are first tabulated in Table III. For the case of *Even Cost*, among all classifiers, the sensitivity, specificity, and accuracy are around 40%, 90%, and 70% with the ECG feature set, whereas they are 60%, 90%, and 80% with the SpO_2 feature set, respectively. To enhance the sensitivity, via testing different penalty weights, we choose a cost matrix to penalize the FN three times that of the FP (i.e., *Cost Sensitive 3*), at the expense of specificity but still maintaining an acceptable accuracy (around 70–80%). Under the *Cost Sensitive 3* section of Table III, the sensitivity of the ECG feature set now ranges from 53.91% to 72.47% and that of the SpO_2 feature set spans over $[70.31\%,\ 87.63\%]$. The accuracies of using these two feature sets remain around 70% and 80%, respectively.

2) Using Combined ECG and SpO_2 Feature Set: Table IV provides both the even cost and cost-sensitive classification results based on the combined feature set. Given the *Cost Sensitive 3* result in Table IV, among ten classifiers, *AdaBoost with Decision Stump* achieves the highest sensitivity of 87.03% but the lowest specificity (74.82%) and accuracy (77.79%). *Bagging with REPTree* enjoys both the highest specificity (85.89%) and accuracy (84.40%) but a relatively low sensitivity (79.75%).

In addition, we record in Table IV the CPU time[2] spent on training and testing of each classifier during the tenfold cross validation. As can be seen, *MLP, Bagging with ADTree, and SVM* are the most computationally intensive classifiers based on the CPU time spent on training: from about 33 to 886 s, whereas the remaining classifiers require no more than 15 s in training.

[2]The aforementioned results are obtained from a PC of a Linux system with Intel Core 2 Duo CPU E6850 @ 3.00 GHz, 2G RAM. All the classifiers are implemented in Java.

TABLE V
SELECTED FEATURES OF REDUCED FEATURE SET FS39

Selected ECG features (8)	*SCrC2, rrff3, rrff4, rrff5, rrff6, edrw2, edrw9, edrf5*
Selected SpO_2 features (31)	*Svari, Smini, NumZC, Dmean, ODIS2, ODIS3, ODIS4, ODIS5, ODI21, ODI23, ODI25, ODI31, ODI35, ODI41, ODI43, ODI45, ODI51, ODI53, ODI55, odi2, odi3, odi4, tsa95, tsa90, tsa85, CTM25, CTM50, CTM75, CTM100, LZCom, ApEnt*

TABLE VI
CLASSIFICATION RESULT OF REDUCED FEATURE SET FS39 WITH COST SENSITIVE 3

	Sen.(%)	Spe.(%)	Acc.(%)	Training Time (s)	Testing Time (s)
SVM	78.88	82.57	81.68	11.162	0.645
C4.5 tree	69.44	84.25	80.64	0.775	0.002
Bagging.REPTree	79.05	**84.62**	**83.26**	2.184	0.001
Bagging.ADTree	83.93	79.45	80.54	14.837	0.006
FT trees	69.81	80.44	77.86	3.672	0.852
AdaBoost	**86.81**	74.54	77.53	0.613	0.001
REPTree	79.65	82.02	81.44	0.230	0.002
kNN ($k = 5$)	78.45	81.77	80.96	0.000	2.085
DecisionTable	81.11	80.83	80.90	2.701	0.002
MLP	77.15	81.11	80.14	70.965	0.013

B. Feature Selection

Applying the feature selection strategy described in Section II-D, 39 out of 150 features are selected as a reduced feature set (FS39) which consists of 8 ECG features and 31 SpO_2 features. In particular, the eight ECG features [11] are the second-order serial correlation coefficient (*SCrC2*), the third, fourth, fifth, and sixth discrete Fourier transform (DFT) points of RR intervals (*rrff3, rrff4, rrff5, rrff6*), the spectral variances of second and ninth levels of decimated wavelet transform of EDR series (*edrw2, edrw9*), and the fifth DFT point of EDR series (*edrf5*). All the selected 39 features are listed in Table V.

Cost-sensitive classifications are carried out to assess the performance of the reduced feature set FS39 and the results are shown in Table VI. Compared with Table IV, using FS39, the computational load shrinks to around only 1/5 of the one using the full combined feature set, for almost all classifiers, with less than 1% decrease in sensitivity, specificity, and accuracy. *AdaBoost with Decision Stump* still achieves the highest sensitivity of 86.81% while *Bagging with REPTree* retains the highest specificity of 84.62% and the accuracy of 83.26% among ten classifiers. In terms of computational efficiency, *SVM*, *Bagging with ADTree*, and *MLP* still consume the longest CPU time (11–71 s on training) while other classifiers only spend less than 3.7 s on training in 1tenfold cross validation.

C. Classifier Combination

The result in the previous section (see Table VI) also shows that although *AdaBoost with Decision Stump* achieves the highest sensitivity, its specificity is the lowest among ten classifiers; *Bagging with REPTree* attains the highest specificity but its sensitivity is below 80%. In the interest of a well-rounded classification result, we apply classifier combination proposed in Section II-E to balance the performances in both sensitivity and specificity, and hence the accuracy.

Since *AdaBoost with Decision Stump* and *Bagging with REPTree* achieve highest sensitivity and specificity, respectively, we choose them as two permanent member classifiers in our combination experiment. On the other hand, to avoid too much computation, three most computationally intensive classifiers: *SVM*, *Bagging with ADTree*, and *MLP* are excluded. As a result, an additional classifier is drawn from the remaining five classifiers sequentially to form a group of three experts. The reduced feature set FS39 and the SpO_2 feature set are both considered in the classifier combination experiment.

Via a thorough experiment with five different choices of the third member classifier, it is found that *kNN* ($k = 5$) and *Decision Table* collaborate best with *AdaBoost with Decision Stump* and *Bagging with REPTree*. Their combination results are illustrated in Tables VII and VIII, respectively. As we can see, the sensitivity, specificity, and accuracy are all around 82% and 81% for the FS39 feature set and the SpO_2 feature set, respectively, for all four combination schemes.

IV. DISCUSSION

A. Comparison Among Different Feature Sets

Recall that in Section III-A1, if we compare the individual signals, the proposed SpO_2 feature set achieves a much better performance than the ECG feature set in both even cost and cost-sensitive cases: averagely, about 25% and 12% advantage in sensitivity and 6% and 8% advantage in accuracy for *Even Cost* and *Cost Sensitive 3*, respectively. Besides, in the selected feature set FS39, the majority existence of SpO_2 features (31 SpO_2 features versus 8 ECG features) also implies the higher diagnostic ability of SpO_2 features than the ECG features. The reason could be explained as follows. Since the SpO_2 signal is a direct reflection of the amount of oxygen that one inhales, it could directly capture the oxygen variation due to the pause/reduction of breath when sleep apnea/hypopnea happens. On the other hand, the ECG signal records the electrical activity of the heart where not only apnea/hypopnea, but also many other metabolic processes as well as, highly possibly, other heart-related disorders are taking place. In this sense, the ECG signal is more complicated and the most sleep-apnea/hypopnea-relevant information might be buried in other signals. Hence, to unveil and extract the most indicative features from ECG for SAHS detection is very challenging. Consequently, if only one sensor is allowed for SAHS detection, oximeter is preferable over ECG sensor.

Moreover, if both ECG and SpO_2 signals are available, using the combined full feature set (see Table IV) can largely improve the performance of using ECG features alone (see Table III): about 15%, 6%, and 7% increases in maximum sensitivity, specificity, and accuracy among ten classifiers, respectively. The reduced feature set FS39, obtained by our proposed cost-sensitive subset feature selection, achieves approximately the same good classification result but only requires about 1/5 of the computational load of the full feature set. Comparing FS39 and the SpO_2 feature set, from Tables VII and VIII, for every combination scheme, FS39 shows advantage (about 1%) over the SpO_2 feature set in sensitivity and accuracy while most of the time in specificity as well. In other words, the incorporation

TABLE VII
PERFORMANCES OF A CLASSIFIER COMBINATION WITH FS39 AND SpO_2 FEATURE SETS

Cost Sensitive 3	Max Prob.		Average Prob.		Product Prob.		Majority Voting	
Bagging.REPTree + AdaBoost + kNN	FS39	SpO_2	FS39	SpO_2	FS39	SpO_2	FS39	SpO_2
Sensitivity (%)	81.87	81.60	82.41	81.71	82.19	81.38	**83.55**	82.41
Specificity (%)	82.07	81.07	82.03	81.21	82.16	81.23	81.25	80.62
Accuracy (%)	82.02	81.20	82.12	81.33	82.16	81.27	81.81	81.05
CPU Time Training (s)	2.991	2.902	2.814	2.893	2.794	2.909	2.927	2.903
CPU Time Testing (s)	2.291	1.987	2.115	1.994	2.074	1.980	2.262	1.993

TABLE VIII
PERFORMANCES OF ANOTHER CLASSIFIER COMBINATION WITH FS39 AND SpO_2 FEATURE SETS

Cost Sensitive 3	Max Prob.		Average Prob.		Product Prob.		Majority Voting	
Bagging.REPTree + AdaBoost + Decision Table	FS39	SpO_2	FS39	SpO_2	FS39	SpO_2	FS39	SpO_2
Sensitivity (%)	82.14	81.82	82.68	82.41	82.57	82.25	**83.61**	82.90
Specificity (%)	81.47	80.69	81.35	80.48	81.42	80.57	80.16	80.43
Accuracy (%)	81.64	80.96	81.68	80.95	81.70	80.98	81.00	81.03
CPU Time Training (s)	5.561	5.156	5.597	5.144	5.581	5.162	5.550	5.149
CPU Time Testing (s)	0.003	0.004	0.004	0.005	0.002	0.003	0.004	0.004

of ECG features complements SpO_2 features by providing additional useful information for SAHS detection. Therefore, with access to both signals, such as in hospital, classifier combination with feature set FS39 serves as a good candidate for real-time SAHS detection. However, given a home-based setting with consideration of the cost of extra sensor, classifier combination based on the SpO_2 signal alone also suffices to offer a decent performance.

B. Comparison Among Different Classification Strategies

Among the ten individual classifiers, *AdaBoost with Decision Stump* achieves the highest sensitivity and *Bagging with REPTree* attains the highest specificity and accuracy almost for all feature sets.

With classifier combination (see Tables VII and VIII), almost all three metrics improve if compared with the results of individual classifiers for both FS39 and SpO_2 feature sets (Tables VI and III): the sensitivity increases at least 2% compared with *Bagging with REPTree* while about 7–8% improvement in specificity and 4–5% increase in accuracy compared with *AdaBoost with Decision Stump*. Conclusively, better and more balanced detection results are achieved with the proposed classifier combination.

Among four different classifier combination schemes, *Majority Voting* always wins the highest sensitivity. Because each member classifier is already in favor of positive class due to the cost-sensitive setting, the final prediction of *Majority Voting* further emphasizes the sensitivity by its "hard decision" nature: based on the classes instead of the associated probabilities.

Given a real-time detection problem, the computational complexity is of concern. *AdaBoost with Decision Stump* and *Bagging with REPTree* are computationally efficient compared to other algorithms such as *SVM* and *MLP*, in addition to their good detection performances. With the two being permanent members for classifier combination, choosing either *kNN* or *Decision Table* as the third member gives comparable classification results as shown in Tables VII and VIII. The difference mainly lies in the computational loads of training and testing. In general, the total training/testing time for the combination approach is the sum of those for individual classifiers. Note that *kNN* is a lazy classifier that requires no time on training; thus, the total training time for the combination approach with *kNN* stays around 2.9 s versus 5.3 s for the combination approach with *Decision Table*. However, since *kNN* offloads the complexity to testing phase, the corresponding testing time of the former is about 2 s, while the latter requires much less, around 3 ms. As a result, the former combination is more suitable for a subject-dependent (SD) application where testing is conducted based on the model trained by the same subject's historical data. In this case, trainings need to be carried out or updated on a subject basis. The latter combination with *Decision Table* fits better for a subject-independent (SI) application where training is already done based on some (large) database before distributing to users who are only responsible for testing.

Regarding the memory requirement of our proposed classifier combination for real-time SAHS detection, both training and testing programs run freely within the default maximum allocated memory (455 MB) which is less than the memory size of iPhone 4 (512 MB RAM). The memory usage for the testing phase of our proposed algorithm is much less since each time only 1 min of data are processed. In addition, for the training process which generally requires more memory, current technology allows large amount of computations to be offloaded to servers via Internet (cloud computing) [11]. As a result, the memory issues can be effectively solved.

Finally, it is interesting to note that performances of algorithms such as *SVM* and *MLP* also depend on parameter settings. However, it is usually unknown beforehand which parameter setting is the best for a given problem. Locating the optimal parameter setting is often done by cross validation and grid search [36]. It is also highly probable that the best parameter setting for one database fails to cater for another database.

Therefore, reoptimization of parameters is required for these algorithms. To avoid such tedious and database-dependent parameter optimization processes, we consider and mainly focus on some other classifiers that require few, if any, parameter adjustments, especially the algorithms chosen for our proposed combination scheme: decision-tree-based algorithms, *Decision Table*, and lazy classifier *kNN*. The relief from parameter optimization also potentially extends the applicability of our proposed scheme to other databases.

C. Comparison With Other Related Works

As mentioned before, most precedent SAHS detection approaches gave overall diagnoses on whether a suspect is with or without SAHS based on the whole overnight signals [5]–[10], [13]–[18]. Several works also developed techniques to detect SAHS on an epoch basis [8]–[12], [19]–[21]. In general, the specific classification results are database-dependent. Some works used their own clinical data [12], [15]–[18]. For instance, Heneghan *et al*. [12] applied linear discriminant analysis for classification with eight ECG features and five SpO_2 features and obtained epoch-wise sensitivity and specificity of 51.4% and 87.3%, respectively. Others [8]–[11], [20] utilized some free online databases from PhysioNet, for example, *Apnea-ECG database* [37] which is the database used in *Computers in Cardiology 2000 Challenge* of sleep apnea detection based on ECG. Two top teams [8], [9] in this challenge achieved above 90% accuracy on an epoch basis where manual inspection was used to identify the apneic episodes in [8] while [9] also relied on manual editing to improve the performances.

Among the most recent automated real-time SAHS detection approaches, Bsoul *et al*. [11] employed SVM for classification based on a very comprehensive ECG feature set. A sensitivity of 96% was attained in the SD experiment while an accuracy of 86% was reported for the SI experiment based on *Apnea-ECG database*. However, as can be seen from Table III, the sensitivity, specificity, and accuracy of the SI experiment are around 67%, 73%, and 71% using SVM with the ECG features proposed by Bsouls *et al*. in *UCD database*. Burgos *et al*. [20] considered data mining techniques and used eight SpO_2 features for real-time SAHS detection. An accuracy of 93% is obtained on *Apnea-ECG database* but it contains only eight subjects' overnight SpO_2 recordings. Applying Burgos' method on *UCD database*, only about 34% sensitivity is returned [21].

Our real-time SAHS detection is carried out on *UCD database* where 25 sleep-disordered-breathing suspects' ECG and SpO_2 signals are both available. We investigate the diagnostic abilities of these two signals individually and in combination. According to our results, our proposed SpO_2 features demonstrate a better detection ability of SAHS than the ECG features. In addition, instead of evaluating the features separately [11], [20], [21], we apply subset feature evaluation in a cost-sensitive manner for feature selection. The selected feature set FS39 is not only of high sensitivity but also of low redundancy among features. More importantly, based on investigations of ten machine-learning algorithms, we propose classifier combination to harness the advantages of individual classifiers and further improve and balance the classification performance, achieving sensitivity, specificity, and accuracy all around 82%.

V. Conclusion

This paper studies the real-time SAHS detection based on ECG and SpO_2 signals, both alone and in combination. According to the tenfold cross-validation result based on ten individual classifiers, our proposed SpO_2 features demonstrated a better diagnostic ability than ECG features. Through a cost-sensitive subset feature selection, a reduced feature set (FS39) of 8 ECG features and 31 SpO_2 features is obtained. Classifier combination is proposed to balance and further improve the performance. It is found that two groups of classifier collaboration stand out among others. Classifier combination based on SpO_2 features only is able to provide a satisfactory detection performance. Nevertheless, given the available ECG signal, adding certain ECG features (as those in FS39) is beneficial to the detection performance.

Acknowledgment

The authors thank the editor and anonymous reviewers for their constructive comments to enhance the quality and presentation of this paper. The authors would like to thank Dr. Majdi Bsoul for providing Matlab codes for [11].

References

[1] T. Young, M. Palta, J. Dempsey, J. Skatrud, S. Weber, and S. Badr, "The occurrence of sleep-disordered breathing among middle-aged adults," *New Engl. J. Med*., vol. 328, no. 17, pp. 1230–1235, 1993.

[2] T. Young, L. Evans, L. Finn, and M. Palta, "Estimation of the clinically diagnosed proportion of sleep apnea syndrome in middle-aged men and women," *Sleep*, vol. 20, no. 9, pp. 705–706, 1997.

[3] S. Ancoli-Israel, E. R. DuHamel, C. Stepnowsky, R. Engler, M. Cohen-Zion, and M. Marler, "The relationship between congestive heart failure, sleep apnea, and mortality in older men," *Chest*, vol. 124, no. 4, pp. 1400–1405.

[4] W. Lee, S. Naqubadi, and M. H. Mokhlesi, "Epidemiology of obstructive sleep apnea: A population-based perspective," *Expert Rev. Respir. Med*., vol. 2, no. 3, pp. 349–364, Jun. 2008.

[5] U. Magalang, J. Dmochowski, S. Veeramachaneni, A. Draw, M. Mador, A. El-Solh, and B. Grant, "Prediction of the apnea-hypopnea index from overnight pulse oximetry," *Chest*, vol. 124, no. 5, pp. 1694–1701, 2003.

[6] N. Netzer, R. Stoohs, C. Netzer, K. Clark, and K. Strohl, "Using the Berlin Questionnaire to identify patients at risk for the sleep apnea syndrome," *Ann. Int. Med*., vol. 131, no. 7, pp. 485–491, 1999.

[7] A. Ng, T. Koh, E. Baey, and K. Puvanendran, "Speech-like analysis of snore signals for the detection of obstructive sleep apnea," in *Proc. Int. Conf. Biomed. Pharmaceut. Eng*., 2006, pp. 99–103.

[8] J. McNames and A. Fraser, "Obstructive sleep apnea classification based on spectrogram patterns in the electrocardiogram," in *Proc. Comput. Cardiol*., 2000, pp. 749–752.

[9] B. Raymond, R. Cayton, R. Bates, and M. Chappell, "Screening for obstructive sleep apnoea based on the electrocardiogram—The computers in cardiology challenge," in *Proc. Comput. Cardiol*., 2000, pp. 267–270.

[10] Z. Shinar, A. Baharav, and S. Akselrod, "Obstructive sleep apnea detection based on electrocardiogram analysis," in *Proc. Comput. Cardiol*., 2000, pp. 757–760.

[11] M. Bsoul, H. Minn, and L. Tamil, "Apnea MedAssist: Real-time sleep apnea monitor using single-lead ECG," *IEEE Trans. Inf. Technol. Biomed*., vol. 15, no. 3, pp. 416–427, May 2011.

[12] C. Heneghan, C. Chua, J. Garvey, P. De Chazal, R. Shouldice, P. Boyle, and W. McNicholas, "A portable automated assessment tool for sleep apnea using a combined Holter-oximeter," *Sleep*, vol. 31, no. 10, pp. 1432–1439, 2008.

[13] P. Lévy, J. Pépin, C. Deschaux-Blanc, B. Paramelle, and C. Brambilla, "Accuracy of oximetry for detection of respiratory disturbances in sleep apnea syndrome," *Chest*, vol. 109, no. 2, pp. 395–399, 1996.
[14] L. Olson, A. Ambrogetti, and S. Gyulay, "Prediction of sleep-disordered breathing by unattended overnight oximetry," *J. Sleep Res*., vol. 8, no. 1, pp. 51–55, 1999.
[15] C. Lin, C. Yeh, C. Yen, W. Hsu, and L. W. Hang, "Comparison of the indices of oxyhemoglobin saturation by pulse oximetry in obstructive sleep apnea hypopnea syndrome," *Chest*, vol. 135, no. 1, pp. 86–93, 2008.
[16] R. Hornero, D. Alvarez, D. Abasolo, F. del Campo, and C. Zamarron, "Utility of approximate entropy from overnight pulse oximetry data in the diagnosis of the obstructive sleep apnea syndrome," *IEEE Trans. Biomed. Eng*., vol. 54, no. 1, pp. 107–113, Jan. 2007.
[17] D. Alvarez, R. Hornero, D. Abásolo, F. Campo, and C. Zamarrón, "Nonlinear characteristics of blood oxygen saturation from nocturnal oximetry for obstructive sleep apnoea detection," *Physiol. Meas*., vol. 27, pp. 399–412, 2006.
[18] C. Zamarrón, F. Gude, J. Barcala, J. Rodriguez, and P. Romero, "Utility of oxygen saturation and heart rate spectral analysis obtained from pulse oximetric recordings in the diagnosis of sleep apnea syndrome," *Chest*, vol. 123, no. 5, pp. 1567–1576, 2003.
[19] N. Oliver and F. Flores-Mangas, "HealthGear: A real-time wearable system for monitoring and analyzing physiological signals," in *Proc. Body Sensor Netw.*, 2006, pp. 61–64.
[20] A. Burgos, A. Goñi, A. Illarramendi, and J. Bermudez, "Real-time detection of apneas on a PDA," *IEEE Trans. Inf. Technol. Biomed*., vol. 14, no. 4, pp. 995–1002, Jul. 2010.
[21] B. Xie, W. Qiu, H. Minn, L. Tamil, and M. Nourani, "An improved approach for real-time detection of sleep apnea," in *Proc. Int. Conf. Bio-Inspired Syst. Signal Process*., 2011, pp. 169–175.
[22] *St. Vincent's University Hospital/University College Dublin Sleep Apnea Database*. (2008). [Online]. Available: http://www.physionet.org/pn3/ucddb/
[23] A. L. Goldberger, L. A. N. Amaral, L. Glass, J. M. Hausdorff, P. C. Ivanov, R. G. Mark, J. E. Mietus, G. B. Moody, C.-K. Peng, and H. E. Stanley, "PhysioBank, PhysioToolkit, and PhysioNet: Components of a new research resource for complex physiologic signals," *Circulation*, vol. 101, no. 23, pp. e215–e220, 2000.
[24] M. Hall, E. Frank, G. Holmes, B. Pfahringer, P. Reutemann, and I. Witten, "The WEKA data mining software: An update," *ACM SIGKDD Explorat. Newslett*., vol. 11, no. 1, pp. 10–18, 2009.
[25] C.-C. Chang and C.-J. Lin. (2001). *LIBSVM: A library for support vector machines* [Online]. Available: http://www.csie.ntu.edu.tw/∼cjlin/libsvm
[26] D. Aha and D. Kibler, "Instance-based learning algorithms," *Mach. Learn*., vol. 6, pp. 37–66, 1991.
[27] R. Kohavi, "The power of decision tables," in *Proc. 8th Eur. Conf. Machine Learning*, 1995, pp. 174–189.
[28] T. M. Mitchell, *Machine Learning* (McGraw Hill Series in Computer Science). New York: McGraw-Hill, 1997.
[29] R. Quinlan, *C4.5: Programs for Machine Learning*. San Mateo, CA: Morgan Kaufmann, 1993.
[30] N. Landwehr, M. Hall, and E. Frank. (2005, May). Logistic model trees. *Mach. Learn*. [Online]. *59*, pp. 161–205. Available: http://dx.doi.org/10.1007/s10994-005-0466-3
[31] Y. Freund and R. E. Schapire, "Experiments with a new boosting algorithm," in *Proc. 13th Int. Conf. Mach. Learn*., 1996, pp. 148–156.
[32] L. Breiman, "Bagging predictors," *Mach. Learn*., vol. 24, no. 2, pp. 123–140, 1996.
[33] Y. Freund, "The alternating decision tree learning algorithm," in *Proc. 6th Int. Conf. Mach. Learn*., 1999, pp. 124–133.
[34] M. A. Hall, "Correlation-based feature subset selection for machine learning" Ph.D. dissertation, Univ. Waikato, Hamilton, New Zealand, 1998.
[35] S. Tulyakov, S. Jaeger, V. Govindaraju, and D. Doermann, *Review of Classifier Combination Methods*. vol. 90. Berlin/Heidelberg, Germany: Springer-Verlag, 2008, pp. 361–386.
[36] C.-W. Hsu, C.-C. Chang, and C.-J. Lin. (2010). "A practical guide to support vector classification," [Online]. Available: http://www.csie.ntu.edu.tw/∼cjlin/libsvm
[37] "CinC Challenge 2000 data sets: Data for development and evaluation of ECG-based apnea detectors," (2000). [Online]. Available: http://www.physionet.org/physiobank/database/apnea-ecg/

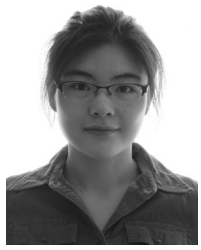

Baile Xie (S'11) received the B.S. degree in communications engineering from the University of Electronic Science and Technology of China, Chengdu, China, in 2008.

She is currently working toward the Ph.D. degree in electrical engineering at the University of Texas at Dallas, Richardson. Her research interests include wireless communications, signal processing, and wireless health-care technologies.

Hlaing Minn (S'99–M'01–SM'07) received the B.E. degree in electronics from the Yangon Institute of Technology, Yangon, Myanmar, in 1995, the M.Eng. degree in telecommunications from the Asian Institute of Technology, Pathumthani, Thailand, in 1997, and the Ph.D. degree in electrical engineering from the University of Victoria, Victoria, BC, Canada, in 2001.

He was a Postdoctoral Fellow at the University of Victoria from January to August of 2002. In September 2003, he joined the Erik Jonsson School of Engineering and Computer Science, University of Texas at Dallas, Richardson, where he is currently an Associate Professor. His research interests include wireless communications, statistical signal processing, error control, detection, estimation, synchronization, signal design, cross-layer design, cognitive radios, and wireless health-care applications.

Dr. Minn is an Editor for the IEEE TRANSACTIONS ON COMMUNICATIONS and *International Journal of Communications and Networks*. He served as a Co-Chair of the Wireless Access Track in the IEEE VTC 2009 (Fall) and as a member of technical program committee in several IEEE major conferences.